3444 Vol. 46, No. 14 / 15 July 2021 / Optics Letters Letter

Optics Letters

Tunable Doppler shift using a time-varying epsilon-near-zero thin film near 1550 nm

Cong Liu,[1,2,*] M. Zahirul Alam,[3,4] Kai Pang,[1] Karapet Manukyan,[1] Joshua R. Hendrickson,[5] Evan M. Smith,[5,6] Yiyu Zhou,[4] Orad Reshef,[3] Hao Song,[1] Runzhou Zhang,[1] Haoqian Song,[1] Fatemeh Alishahi,[1] Ahmad Fallahpour,[1] Ahmed Almaiman,[7] Robert W. Boyd,[3,4] Moshe Tur,[8] and Alan E. Willner[1]

[1]Department of Electrical Engineering, University of Southern California, Los Angeles, California 90089, USA
[2]Department of Physics and Astronomy, University of Southern California, Los Angeles, California 90089, USA
[3]Department of Physics, University of Ottawa, Ottawa, ON K1N 6N5, Canada
[4]University of Rochester, Rochester, New York 14642, USA
[5]Air Force Research Laboratory, Sensors Directorate, Wright-Patterson AFB, Dayton, Ohio 45433, USA
[6]KBRwyle Laboratories, Beavercreek, Ohio 45431, USA
[7]King Saud University, Riyadh, Saudi Arabia
[8]School of Electrical Engineering, Tel Aviv University, Ramat Aviv 69978, Israel
*Corresponding author: liucong@usc.edu

Received 30 April 2021; revised 16 June 2021; accepted 17 June 2021; posted 17 June 2021 (Doc. ID 430106); published 14 July 2021

We experimentally investigate the tunable Doppler shift in an 80 nm thick indium-tin-oxide (ITO) film at its epsilon-near-zero (ENZ) region. Under strong and pulsed excitation, ITO exhibits a time-varying change in the refractive index. A maximum frequency redshift of 1.8 THz is observed in the reflected light when the pump light has a peak intensity of ∼140 GW/cm^2 and a pulse duration of ∼580 fs, at an incident angle of 40°. The frequency shift increases with the increase in pump intensity and saturates at the intensity of ∼140 GW/cm^2. When the pump pulse duration increases from ∼580 fs to ∼1380 fs, the maximum attainable frequency shift decreases from 1.8 THz to 0.7 THz. In addition, the pump energy required to saturate the frequency shift decreases with the increase in pump pulse duration for ≲1 ps and remains unchanged for ≳1 ps durations. Tunability exists among the pump pulse energy, duration, and incident angle for the Doppler shift of the ITO-ENZ material, which can be employed to design efficient frequency shifters for telecom applications.

https://doi.org/10.1364/OL.430106

Materials containing free charges, such as highly doped semiconductors, can exhibit a zero real part of permittivity at their bulk plasmon wavelength (zero-permittivity wavelength, λ_{zero}) [1]. These materials, known as epsilon-near-zero (ENZ) materials, have a near-zero linear refractive index near λ_{zero} due to the vanishingly small real permittivity value. This region near λ_{zero} is referred to as the ENZ region of the material. Such ENZ materials are reported to exhibit unique linear and strong nonlinear properties [1–10]. Based on their strong nonlinear optical responses, ENZ materials may be suitable candidates for exploiting various reconfigurable applications, such as high-speed optical switching, optical signal processing, dynamic routing, and broadband frequency shifting [11–14].

A subwavelength-thick indium-tin-oxide (ITO) material, as one example of ENZ materials, has been reported to possess an ultrafast, large, non-instantaneous, and intensity-dependent time-varying refractive index change [5,6]. The induced time-varying refractive index can then shift the optical frequency of a sub-picosecond pulsed excitation beam by up to terahertz (i.e., tens of nanometers in wavelength) in a sub-micrometer thick ENZ material [7,8]. This frequency shift is analogous to the Doppler shift of light arising from a moving boundary [7,15,16].

The nonlinear frequency shift utilizing time-varying ENZ materials has been previously demonstrated: (i) an up to ∼2.8 THz frequency shift was induced in a 900 nm thick aluminum-doped zinc oxide film when pumped at λ_{zero} of 1250 nm [7], and (ii) an up to 14.9 THz frequency shift was observed in a 620 nm thick ITO film when pumped near its λ_{zero} of 1240 nm [8]. However, there have been few reports describing such nonlinear frequency shifts in the "telecom C band" ∼1550 nm. Therefore, it could be of interest to explore the nonlinear optical effects, such as Doppler shift of light in an ENZ material in this wavelength region.

In this paper, we experimentally demonstrate tunable Doppler shifts in the reflected light from an 80 nm thick ITO-ENZ film. The ITO film is pumped with pulsed light centered near its ENZ region (i.e., ∼1550 nm). We observe a tunable frequency redshift in the spectra of light reflected from the ITO film with a maximum value of 1.8 THz when the pump light has a ∼140GW/cm^2 peak intensity (where the shift saturates), a ∼580 fs pulse duration, and a 40° incident angle. The maximum attainable frequency shift decreases from 1.8 THz to 0.7 THz when the pump pulse duration increases from ∼580 fs

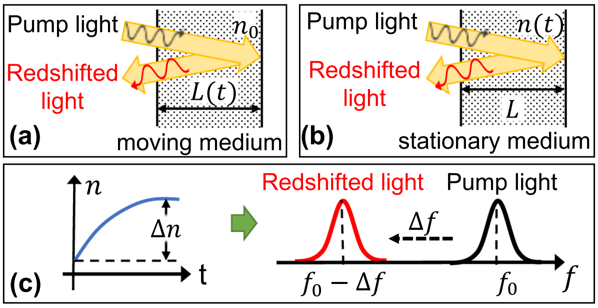

Fig. 1. Concept of Doppler shift. A Doppler shift can be induced when light is reflected by (a) moving medium with a fixed refractive index n_0 or (b) stationary medium with a time-varying refractive index $n(t)$. (c) In the latter case, the refractive index change (Δn) of the medium results in a frequency shift Δf in light. L, medium thickness.

to ~1380 fs. Moreover, for ≲1 ps pulse duration, the saturation energy of the frequency shift for the ITO film decreases with the increase in pump pulse duration. This saturation intensity remains almost constant for ≳1 ps pulse durations. When comparing our experiment to commercial state-of-art frequency shifters such as acousto-optic frequency shifters (AOFSs), the following are observed: (i) AOFS changes the frequency of a beam by gigahertz and requires acousto-optic crystal of millimeter thickness [17]; and (ii) our result achieves three orders of magnitude larger frequency shift by using a four orders of magnitude thinner ITO material. Previously, Alam *et al.* [6] investigated the self-phase modulation in ENZ material using the spatial distortion of light. In this study, we investigate the manifestation of this effect in both time and frequency domains, specifically in reflection geometry. The pulse intensity, incident angle, and duration could be used as "knobs" for controlling the frequency shift amount introduced by the time-varying ITO-ENZ film.

A Doppler shift can arise from light reflected by: (i) a medium with a moving boundary and fixed refractive index n_0 [Fig. 1(a)] or (ii) a stationary medium with a time-varying refractive index $n(t)$ [Fig. 1(b)], which are identical to each other. In (ii), the constant phase plane experiences a phase shift ϕ [15,16]:

$$\phi = k_0 n(t) L, \tag{1}$$

where $k_0 = (2\pi f_0/c)$ is the free-space wavenumber of the pump light, and L is the medium thickness. For a thin (sub-micrometer) time-varying medium, the induced frequency shift Δf [7] is

$$\Delta f = \frac{\Delta\omega}{2\pi} = -\frac{1}{2\pi}\frac{\partial\phi}{\partial t} = -\frac{k_0 L}{2\pi}\frac{\mathrm{d}n(t)}{\mathrm{d}t} = -L\frac{\mathrm{d}n(t)}{\mathrm{d}t}\frac{f_0}{c}; \tag{2}$$

with the time-dependent change of $n(t)$ in the material, a Doppler shift could be induced in light [7,18] [Fig. 1(c)].

We design and deposit an 80 nm ITO film by using direct current (DC)-magnetron sputtering at an elevated temperature of 500°C, in an oxygen partial pressure on a z-cut sapphire substrate [Fig. 2(a)]. The λ_{zero} of the ITO can be engineered by tuning the doping density [6,19,20]. We design this λ_{zero} to be ~1550 nm, which is verified by the linear permittivity measurement using ellipsometry, as shown in Fig. 2(b). We define the ENZ region to be the wavelength range where $|Re(\epsilon)| < 0.2$; thus, ~1520 nm to ~1580 nm. The Drude model is used

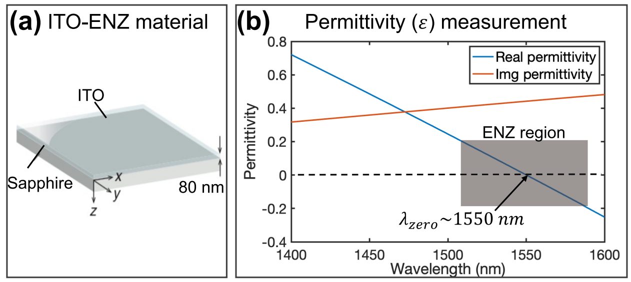

Fig. 2. (a) 80 nm thick ITO film deposited on a sapphire substrate. (b) Linear permittivity of the ITO material measured by spectroscopic ellipsometry, showing $\lambda_{zero} \sim 1550$ nm.

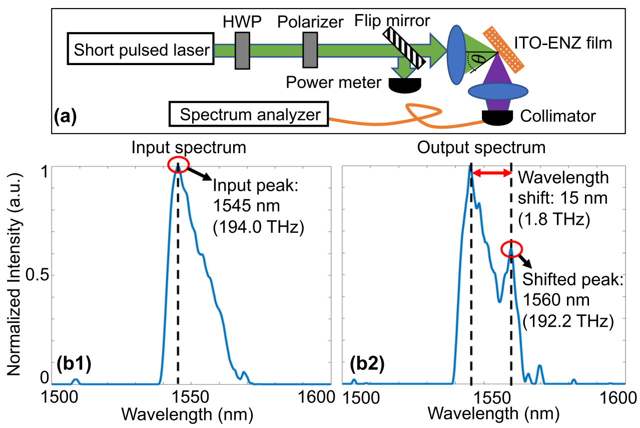

Fig. 3. (a) Experimental setup for the Doppler shift characterization. Examples of (b1) input and (b2) output spectra of the ITO film. The output spectrum shows a maximum attained frequency shift of 1.8 THz. HWP, half-wave plate.

to obtain the complex permittivity. The Drude model gives the resistivity $\rho = 2.55 \times 10^{-4} \Omega \cdot \mathrm{cm}$ with a scattering time $\tau = 7.49 \times 10^{-15}$ s. The carrier concentration and the mobility can be calculated as $n = \frac{m^*}{q^2\tau\rho}$ and $\mu = \frac{q\tau}{m^*}$, respectively, where m^* is the carrier effective mass, and q is the electron charge. The m^* value varies between different ITO samples and in the range of $\sim 0.41 \pm 0.5$ [21,22]. Thus, it is calculated that $n = 7.4 \times 10^{20}\ \mathrm{cm}^{-3}$ and $\mu = 32.9\ \mathrm{cm}^2 \cdot V^{-1} \cdot \mathrm{s}^{-1}$. We collect the n and μ values through Hall effect measurements from a similar ITO sample, and the measured results matches the fitted ρ value from the Drude model [23].

We characterize the Doppler shift, and the experimental setup is shown in Fig. 3(a). A pulsed laser source with a 606 kHz repetition rate and a ~580 fs pulse duration provides the pump light. The laser output light has a spectral wavelength center at ~1550 nm and is polarized parallel to the plane of incidence. The incident power is tuned by using a polarizer and a half-wave plate. We focus the light onto the ITO film to a spot with a ~13 μm diameter using an aspheric lens with an effective focal length of 11 mm. The reflected light from the ITO film is collected by another aspheric lens of the same focal length and a 1 m multimode fiber with a core diameter of 50 μm. An optical spectrum analyzer is used to measure the spectrum. We observe a 1.8 THz maximum frequency shift value in the reflected light at a pump intensity of ~140 GW/cm^2 and an incident angle of 40°. Figures 3(b1) and 3(b2) present the normalized spectra

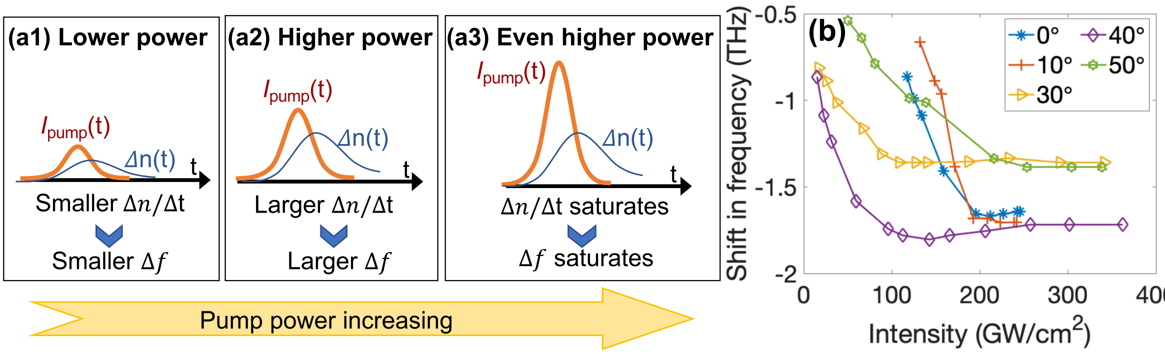

Fig. 4. (a) Illustration of pulse intensity influence on the frequency shift. (a1) A lower pump power leads to a smaller Δn in ITO, resulting in smaller Δf, while (a2) a larger pump power leads to a larger Δf. (a3) The amount of Δn has a limitation due to the free-electron density limitation that Δf saturates with the increase in pump power. (b) Measured Doppler shifts as functions of pump intensity under various incident angles (θ).

of the incident and reflected light, respectively, showing the maximum frequency shift of 1.8 THz. The reflected spectrum has two peaks: the reflected pump light with a center of 1545 nm (∼194.0 THz) and the redshifted light with a center at 1560 nm (∼192.2 THz). The reasons for the two observed peaks in the reflected light might be (i) the ITO thickness is smaller than the longitudinal length of the pulse, and therefore not all of the pulses reside inside the layer at the same instance and the spectrometer measures the time-averaged spectra of the reflected pulse. We hypothesize that the thickness plays a nontrivial role on the frequency shift amount due to thickness-dependent thin film interference effects [5]. (ii) Some of the pump light may be reflected directly from the top surface of the ITO and may not pass through the time-varying ITO medium. (iii) The Δn in the ITO medium induced by the pump light might be delayed in the time domain compared to the pump pulse itself so that some of the pump light does not experience this Δn and cannot be shifted [6].We note that an additional peak around 1580 nm in Fig. 3(b2) is perhaps due to the cascading effect resulting from a fraction of the pulse passing the boundary more than once.

A pulsed pump with a central wavelength λ_{zero} of ITO induces a time-dependent Δn of the ITO film over sub-picosecond time [6,8]. The pump light then interacts with the Δn of the ITO, resulting in the observed frequency shift. According to Eq. 2, the light's frequency shift is proportional to $\frac{dn}{dt}$. When the light experiences a positive Δn during the pulse rising, a redshift in the frequency can be observed. The amount and sign of $\frac{dn}{dt}$ depend on the pump intensity, pump temporal envelope, and the intrinsic nonlinear properties of the ITO material [6,8,9]. For pump pulses with fixed durations, this experiences a fixed time period (Δt), and a higher pump intensity leads to a larger Δn over the same Δt compared with the case of lower pump intensity [Figs. 4(a1)–4(a2)]. In addition, the Δn in the ITO has a limitation due to the limitation of free-electron density inside the ITO medium [24]; thus, $\frac{dn}{dt}$ saturates as Δn reaches the limitation at a certain pump intensity, leading to the saturation of the frequency shift [Fig. 4(a3)]. We characterize the magnitude of the frequency shift as functions of pump intensity for various pump incident angles (θ) as shown in Fig. 4(b), and frequency redshifts are observed. When θ is fixed, the frequency shift increases with the increase in pump intensity until reaching saturation (i.e., the frequency shift amount does not continue to change with the increase in pump intensity). This agrees with

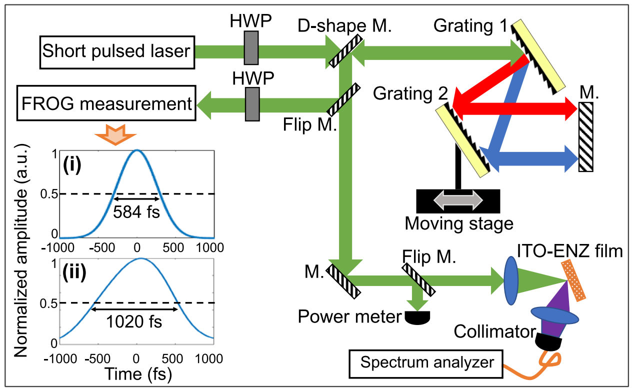

Fig. 5. Experimental setup for modifying the pump pulse duration for measurements in Figs. 6(b)–6(d). Insets (i), (ii): FROG measurement of the pulse: (i) initial pulse and (ii) one stretched pulse. M, mirror; FROG, frequency-resolved optical gating.

the time-dependent Δn explained in Fig. 4(a). In addition, we note that the saturation incident intensity varies with the angle of incidence. We believe this results from an interplay between the field enhancement from the discontinuity of the longitudinal component of the electric field and the angle-dependent Fresnel reflection [6].

To investigate the influence of the pump pulse duration on the Doppler shift effect of ITO, we stretch the pulse duration. The experimental setup is presented in Fig. 5. A pair of diffraction gratings (Richardson Gratings, 53-*-660R) is used to stretch the pulse duration. Between the gratings, different wavelength components in the pulsed light travel with different distances, leading to stretching of the pulses due to the chromatic dispersion of light. This dispersion is measured to be positive and can be tuned by varying the distance between the two gratings using a moving stage. A frequency-resolved optical gating (FROG) is used to measure the stretched pulses in the temporal domain. Figure 5 inset (i) shows the FROG measurement of the original pulse with 584 fs duration, and Fig. 5 inset (ii) shows an example of modifying the pulse to 1020 fs duration. The pulsed light is then focused onto the ITO film using the same aspheric lens as in Fig. 3(a) to achieve the same spot diameter of ∼13 μm. With the same reflected light collection method as in Fig. 3(a), the output light is collected for analysis.

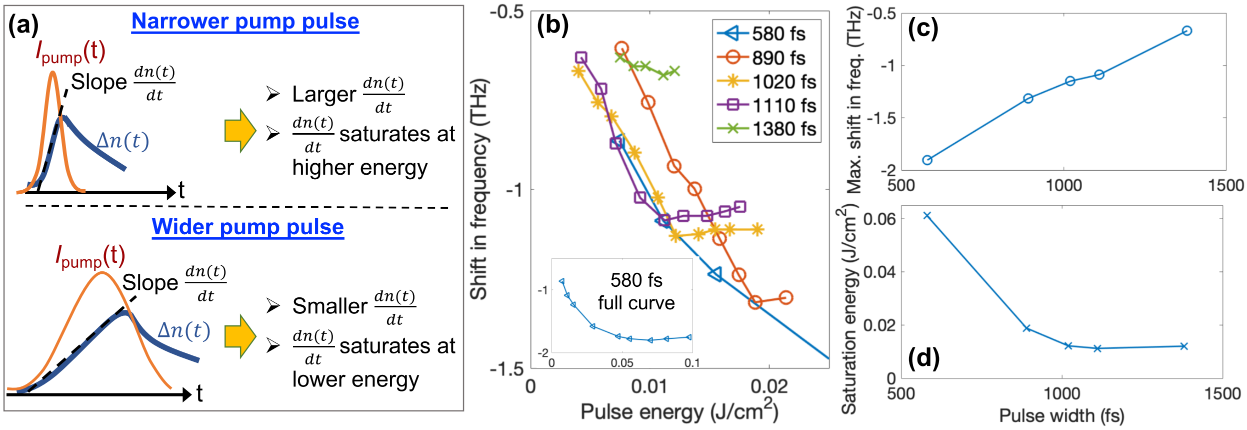

Fig. 6. (a) Illustration of the pump pulse duration influence on the $n(t)$ of ITO. (b) Measured frequency shift as functions of the pump pulse energy. (c) Maximum attainable frequency shifts and (d) frequency shift saturation energy as functions of pump pulse duration.

As presented in Fig. 6(a), a pump pulse with a shorter duration has a larger pulse amplitude changing slope, leading to a larger $\frac{dn}{dt}$ in the ITO material compared to the case of a longer pump pulse duration. Moreover, the saturation of $\frac{dn}{dt}$ would also be reached at a higher pulse energy when the pulses are narrower in the time domain. The Doppler shift amount is relatively proportional to $\frac{dn}{dt}$ in the ITO material. Figure 6(b) presents the measured Doppler shifts under different pump pulse durations. The measurements are taken at an incident angle of 40°, under which the maximum frequency shift is achieved for the original case with 584 fs pulse duration. We find that, for a given pump pulse duration, the frequency shift initially increases with the increase in pulse energy, then saturates, which is similar to the case with the original, unstretched pulse. We note that adding the grating pair introduces extra loss in the setup; thus, the stretched pulse case has lower maximum energy than the original pulse case in Fig. 6(b). The maximum attainable frequency shifts for different pump pulse durations are summarized in Fig. 6(c). When the frequency shift saturates with pump energy, the maximum attainable frequency shift is achieved. This maximum attainable frequency shift decreases almost linearly from 1.8 THz to 0.7 THz when the pump pulse duration increases from ∼580 fs to ∼1380 fs. This may be due to the smaller $\frac{dn}{dt}$ induced by the longer pulse duration. We estimate this close-to-linear decrease from our experimental results. Figure 6(d) shows that the saturation energy of the frequency shift decreases with the increase in pulse duration and remains almost unchanged for pulses longer than 1 ps. This is likely because that $\frac{dn}{dt}$ saturates at a lower pump pulse energy under a wider pulse, and the saturation of $\frac{dn}{dt}$ leads to the saturation of the frequency shift amount with the pulse energy [6,8,9].

Funding. Defense Advanced Research Projects Agency (W911NF-18-0369).

Disclosures. The authors declare no conflicts of interest.

Data Availability. Data underlying the results presented in this paper are not publicly available at this time but may be obtained from the authors upon reasonable request.

REFERENCES

1. N. Engheta, Science **340**, 286 (2013).
2. H. Suchowski, K. O'Brien, Z. J. Wong, A. Salandrino, X. Yin, and X. Zhang, Science **342**, 1223 (2013).
3. A. Alu, M. G. Silveirinha, A. Salandrino, and N. Engheta, Phys. Rev. B **75**, 155410 (2007).
4. L. Caspani, R. Kaipurath, M. Clerici, M. Ferrera, T. Roger, J. Kim, N. Kinsey, M. Pietrzyk, A. Di Falco, V. M. Shalaev, A. Boltasseva, and D. Faccio, Phys. Rev. Lett. **116**, 233901 (2016).
5. O. Reshef, I. De Leon, M. Z. Alam, and R. W. Boyd, Nat. Rev. Mater. **4**, 535 (2019).
6. M. Z. Alam, I. De Leon, and R. W. Boyd, Science **352**, 795 (2016).
7. A. Shaltout, M. Clerici, N. Kinsey, R. Kaipurath, J. Kim, E. G. Carnemolla, D. Faccio, A. Boltasseva, V. M. Shalaev, and M. Ferrera, in *CLEO: QELS_Fundamental Science* (Optical Society of America, 2016), p. FF2D-6.
8. Y. Zhou, M. Z. Alam, M. Karimi, J. Upham, O. Reshef, C. Liu, A. E. Willner, and R. W. Boyd, Nat. Commun. **11**, 1 (2020).
9. C. Liu, M. Z. Alam, K. Pang, K. Manukyan, J. R. Hendrickson, E. M. Smith, Y. Zhou, O. Reshef, H. Song, R. Zhang, and H. Song, in *CLEO: QELS_Fundamental Science* (Optical Society of America, 2020), p. FTu3Q-5.
10. W. Tian, F. Liang, D. Lu, H. Yu, and H. Zhang, Photon. Res. **9**, 317 (2021).
11. M. F. Yanik and S. Fan, Phys. Rev. Lett. **92**, 083901 (2004).
12. V. Bruno, S. Vezzoli, C. DeVault, E. Carnemolla, M. Ferrera, A. Boltasseva, V. M. Shalaev, D. Faccio, and M. Clerici, Appl. Sci. **10**, 1318 (2020).
13. N. Kinsey, C. DeVault, J. Kim, M. Ferrera, V. Shalaev, and A. Boltasseva, Optica **2**, 616 (2015).
14. Y. Yang, K. Kelley, E. Sachet, S. Campione, T. S. Luk, J.-P. Maria, M. B. Sinclair, and I. Brener, Nat. Photon. **11**, 390 (2017).
15. J. Bennett, Aust. J. Phys. **21**, 259 (1968).
16. P. Dyson, J. Atmos. Terr. Phys. **37**, 1151 (1975).
17. C. J. Sarabalis, R. Van Laer, R. N. Patel, Y. D. Dahmani, W. Jiang, F. M. Mayor, and A. H. Safavi-Naeini, Optica **8**, 477 (2021).
18. A. Shaltout, A. Kildishev, and V. Shalaev, Opt. Mater. Express **5**, 2459 (2015).
19. A. Capretti, Y. Wang, N. Engheta, and L. Dal Negro, Opt. Lett. **40**, 1500 (2015).
20. E. Feigenbaum, K. Diest, and H. A. Atwater, Nano Lett. **10**, 2111 (2010).
21. J. W. Cleary, E. M. Smith, K. D. Leedy, G. Grzybowski, and J. Guo, Opt. Mater. Express **8**, 1231 (2018).
22. J. Park, J.-H. Kang, X. Liu, and M. L. Brongersma, Sci. Rep. **5**, 1 (2015).
23. Y. Gui, M. Miscuglio, Z. Ma, M. H. Tahersima, S. Sun, R. Amin, H. Dalir, and V. J. Sorger, Sci. Rep. **9**, 1 (2019).
24. R. Secondo, J. Khurgin, and N. Kinsey, Opt. Mater. Express **10**, 1545 (2020).